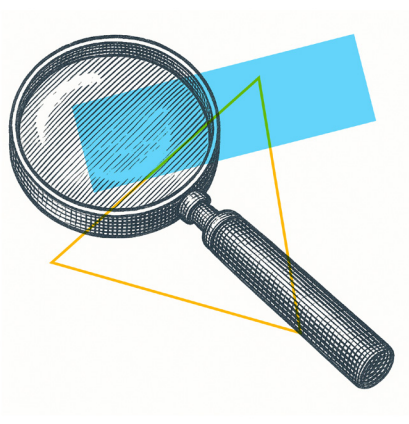


terraFlow's value in early-stage clinical trials

Complete and comprehensive pharmacodynamic analysis of drugs that target the immune system



Pratip K. Chattopadhyay, Ph.D.
Chief Scientific Officer and Co-Founder
terraFlow

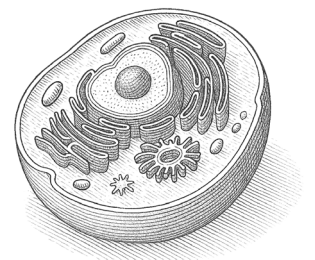
Introduction

Pharmacodynamics is the study of how drugs interact with biological systems to produce their effects. The discipline examines mechanisms of action, the relationship between drug concentration and effect, and how these effects vary across individuals. This field is crucial in drug development as it provides insights into the efficacy and safety profile of a drug. By understanding pharmacodynamics, researchers can optimize therapeutic benefits while minimizing adverse effects. Pharmacodynamic studies also help determine appropriate dosages, identify potential drug interactions, and tailor treatments to specific patient groups. Pharmacodynamic work ensures that new medications meet rigorous standards of effectiveness and safety before reaching the market.

Many new drugs are being developed for use in immuno-oncology and other immune-associated disorders. The molecular targets of these drugs may be proteins on the surface of immune cells, or proteins involved in the interaction between diseased cells (i.e., cancer cells) and immune cells. In either case, this class of drugs is likely to induce an immune response, consisting of cell activation, proliferation, differentiation,

cytokine release, cytotoxicity, and/or downregulation of immune receptors. Studies of these immune changes – usually by flow cytometry – can be very sensitive and informative, since immune responses often serve as a sentinel for broader physiological processes, like inflammation or disease dissemination. Furthermore, identifying exactly which immune cells change during treatment enables a deeper understanding of both the drug's mechanism of action and the underlying disease process.

When we developed terraFlow, our primary focus was to compare patient groups (i.e., responders/non-responders), but we quickly realized that datasets from dose escalation and dose expansion studies are well-suited for terraFlow analyses too. Here, we demonstrate how terraFlow provides key information in the pharmacodynamic analysis of a drug that targets an immunosuppressive pathway tumors use to evade detection by natural killer and T-cells.



Why is terraFlow the right tool for pharmacodynamic studies?

The immune system is a complex network of interconnected cell populations, constantly interacting and influencing each other's differentiation, function, and fate. Although a drug's molecular target may be well-characterized, treatment is likely to have off-target effects—some beneficial, others potentially toxic. Early human studies can interrogate these changes, guide patient selection, and offer a deeper mechanistic understanding of drug effects for later drug development phases.

High-parameter flow cytometry is the most efficient and sensitive tool for detecting treatment-induced immune changes. Antibody panels that simultaneously measure the drug target and other immune populations are among the most powerful tools for pharmacodynamic screening. However, this value can only be realized with the right analytical tools. The best tools comprehensively mine data in an unbiased and automated manner, compute statistics to distinguish real changes from noise, and clearly identify the affected cell populations.

We designed terraFlow to meet these exact requirements. terraFlow analyzes high-parameter flow cytometry data by first identifying cells that express (or lack) a given marker. It then builds phenotypes representing all possible combinations of five markers, calculates the proportion of cells within each phenotype, and iterates this process across combinations of four, three, and two markers—eventually covering the entire data space. It also quantifies the frequency of populations defined by single markers. terraFlow then assesses how each phenotype's frequency correlates with pharmacodynamic outcomes (e.g., dose, time point, adverse event). In sum, terraFlow provides an automated, comprehensive, and unbiased screen

of high-dimensional flow data, initiated via a simple web-based application with results returned within 24 hours.

Gating approaches used by terraFlow

terraFlow offers three methods for determining thresholds (gates) between marker-positive and -negative cells:

- ▶ **User-defined gating:** Used here, this method lets users specify the fluorescence threshold during data upload. Users can also incorporate gating controls such as FMOs.
- ▶ **Automated gating:** For bimodal distributions, gates are placed at the lowest density between peaks. For unimodal distributions, the threshold is set at the right shoulder, where the density drops most steeply.
- ▶ **Non-gating (terraFlow's unique method):** Automatically applied in every analysis, this approach transforms fluorescence intensities along a sigmoidal curve, stretching extreme values and weighting cells that are bright for multiple markers. This produces a weighted transformation that substitutes for frequency data in traditional gating, which is then tested for correlation to pharmacodynamic outcomes. It is particularly appropriate for multi-marker correlates of immunity, like polyfunctional T-cells.

In this dataset, the user-defined approach performed well, likely due to the high-quality cytometry data. When batch variation is present, terraFlow allows users to label batches and assess whether trends differ across them before data is merged. Batch effects were manually evaluated and determined to be minimal in this study, and did not merit the implementation of the batch analysis feature. Review of user-defined gates confirmed that, while marker

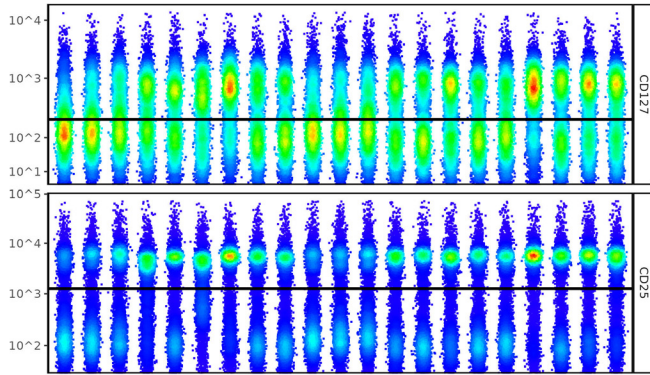


Figure 1: Examples of user-defined thresholds (gates).

expression varied across samples (Figure 1), fluorescence distributions were consistent and thresholds were appropriately placed. These gates were then used to construct phenotypes with all combinations of five to two markers and calculate single-marker frequencies.

Kinetics of T-cell populations by dose

In this study, a 15-color flow cytometry panel was used to evaluate cancer patients enrolled in a Phase I trial of a drug targeting an immunosuppressive tumor pathway. Longitudinal samples were collected over nearly three months. The study included dose escalation (1, 3, 6, and 10 mg/kg) and dose expansion (10 mg/kg in 30 patients) phases.

terraFlow's analysis begins by examining single-marker-defined populations. For each marker, frequencies are shown by time point (columns in Figure 2), with fold change, Co-

hen's statistic (standard deviations between extremes), and adjusted p-values from a paired ANOVA. The values within each cell are the median frequencies of each population (defined by the single marker assigned to that table row; e.g.,

Marker	ZI	1	8	15	22	43	50	57	Fold	Cohens	Pvalue
CD127	14	40.61 ± 5.95%	41.36 ± 3.04%	50.98 ± 6.58%	48.20 ± 7.89%	52.25 ± 19.78%	54.54 ± 13.66%	51.33 ± 0.44%	1.29	2.83	0.587
CD25	6	36.20 ± 8.76%	35.54 ± 1.82%	55.76 ± 16.59%	59.42 ± 3.59%	55.13 ± 25.64%	57.93 ± 13.85%	54.92 ± 3.86%	1.79	6.97	0.143
CD278(COS)	2	8.39 ± 2.64%	11.07 ± 1.29%	11.13 ± 2.34%	9.56 ± 2.38%	11.13 ± 2.38%	10.39 ± 3.82%	9.13 ± 2.34%	1.63	1.44	0.731
CD3	10	13.40 ± 3.67%	11.46 ± 0.95%	28.54 ± 13.36%	26.60 ± 2.38%	28.88 ± 5.18%	33.14 ± 13.81%	27.55 ± 5.64%	2.78	4.76	0.120
CD314	11	26.65 ± 1.64%	23.37 ± 1.81%	41.91 ± 16.48%	41.45 ± 8.38%	44.61 ± 21.47%	46.03 ± 15.27%	41.74 ± 2.53%	1.88	9.99	0.229
CD38	9	35.06 ± 6.94%	33.47 ± 1.90%	49.52 ± 11.35%	52.17 ± 4.56%	52.00 ± 22.52%	54.85 ± 11.60%	51.26 ± 3.86%	1.62	4.10	0.174
CD4	13	20.91 ± 5.72%	20.54 ± 0.33%	35.78 ± 12.14%	31.06 ± 4.56%	33.28 ± 11.82%	41.19 ± 15.98%	37.25 ± 3.21%	1.94	6.24	0.259
CD45	5	35.85 ± 8.76%	35.06 ± 1.75%	55.34 ± 16.75%	59.07 ± 3.54%	54.84 ± 25.63%	57.67 ± 13.96%	54.62 ± 3.91%	1.80	6.89	0.142
CD69	3	52.84 ± 2.79%	51.87 ± 2.84%	52.92 ± 1.79%	48.76 ± 8.50%	57.52 ± 15.36%	59.66 ± 11.82%	57.06 ± 4.48%	1.37	1.19	0.749
CD8	12	12.54 ± 3.89%	10.01 ± 0.74%	20.63 ± 8.72%	17.36 ± 1.79%	22.01 ± 15.96%	23.76 ± 11.82%	16.75 ± 3.21%	2.15	4.31	0.341
FoxP3	7	39.41 ± 6.52%	39.26 ± 2.13%	59.41 ± 16.03%	62.86 ± 4.32%	57.05 ± 25.59%	60.68 ± 13.63%	57.55 ± 3.96%	1.78	7.62	0.157
HLADR	15	37.14 ± 6.73%	34.60 ± 3.09%	48.30 ± 10.85%	46.44 ± 9.74%	49.46 ± 21.98%	52.34 ± 15.47%	49.08 ± 0.17%	1.44	4.13	0.505
Ki67	4	15.16 ± 4.31%	18.68 ± 1.01%	19.42 ± 2.68%	20.73 ± 4.19%	21.14 ± 3.40%	21.85 ± 3.40%	22.94 ± 4.79%	1.64	1.81	0.214

Figure 2: Changes in cells expressing each of the markers in the panel, over the course of treatment with 1mg/kg of the drug (the headers are days on treatment).

CD127+ cells at day 1 have a median frequency of 40.61%, +5.95%); the color coding of the cell allows a quick view of how the data for that marker changes over time. For the 1 mg/kg dose, markers like CD69 and Ki-67 remained relatively unchanged, while others (e.g., FoxP3) increased dramatically (from 39.26% to 59.41%). However, none of these changes were statistically significant over time at the lowest dose.

At 10 mg/kg (Figure 3), significant changes were observed in CD127+, CD3+, CD314+, CD38+, CD4+, CD69+, CD8+, and FoxP3+ populations. Most markers spiked at Day 8, except Ki-67+, which rose gradually around Day 43. A second

1mg/kg												10mg/kg														
Marker	ZI	1	8	15	22	43	50	57	Fold	Cohens	Pvalue	Marker	ZI	1	8	15	22	43	50	57	64	85	Fold	Cohens	Pvalue	
CD127	14	40.61 ± 5.95%	41.36 ± 3.04%	50.98 ± 6.58%	48.20 ± 7.89%	52.25 ± 19.78%	54.54 ± 13.66%	51.33 ± 0.44%	1.29	2.83	0.587	CD127	3	32.69 ± 14.79%	56.98 ± 9.42%	33.46 ± 13.19%	35.25 ± 8.26%	31.18 ± 9.77%	38.04 ± 7.17%	31.13 ± 5.60%	39.02 ± 9.47%	46.17 ± 19.24%	2.15	2.01	0.044	
CD25	6	36.20 ± 8.76%	35.54 ± 1.82%	55.76 ± 16.59%	59.42 ± 3.59%	55.13 ± 25.64%	57.93 ± 13.85%	54.92 ± 3.86%	1.79	6.97	0.143	CD25	15	37.84 ± 25.04%	75.53 ± 10.61%	38.69 ± 24.92%	44.20 ± 11.99%	55.96 ± 21.41%	45.25 ± 8.94%	51.74 ± 13.35%	53.57 ± 13.84%	53.57 ± 13.84%	2.71	2.18	0.123	
CD278(COS)	2	8.39 ± 2.64%	11.07 ± 1.29%	11.13 ± 2.34%	9.56 ± 2.38%	11.13 ± 2.34%	10.39 ± 3.82%	9.13 ± 2.34%	1.63	1.44	0.731	CD278(COS)	2	9.79 ± 5.29%	17.79 ± 6.32%	9.40 ± 2.66%	9.48 ± 2.71%	15.82 ± 4.87%	9.27 ± 3.53%	11.80 ± 4.29%	10.88 ± 7.26%	14.21 ± 7.10%	13.28 ± 7.10%	2.22	3.15	0.194
CD3	10	13.40 ± 3.67%	11.46 ± 0.95%	28.54 ± 13.36%	26.60 ± 2.38%	28.88 ± 5.18%	33.14 ± 13.81%	27.55 ± 5.64%	2.78	4.76	0.120	CD3	6	14.37 ± 9.51%	51.35 ± 13.56%	13.00 ± 10.81%	19.10 ± 9.21%	15.82 ± 10.28%	20.25 ± 7.59%	18.00 ± 7.65%	31.82 ± 11.51%	32.80 ± 17.61%	7.10	2.53	<0.001	
CD314	11	26.65 ± 1.64%	23.37 ± 1.81%	41.91 ± 16.48%	41.45 ± 8.38%	44.61 ± 21.47%	46.03 ± 15.27%	41.74 ± 2.53%	1.88	9.99	0.229	CD314	7	24.96 ± 19.05%	62.61 ± 12.22%	23.04 ± 10.41%	28.97 ± 10.41%	29.32 ± 14.02%	31.87 ± 7.89%	24.22 ± 8.55%	38.84 ± 12.20%	44.63 ± 22.51%	7.27	3.14	0.017	
CD38	9	35.06 ± 6.94%	33.47 ± 1.90%	49.52 ± 11.35%	52.00 ± 3.20%	52.00 ± 11.80%	51.56 ± 5.86%	51.56 ± 5.86%	1.62	4.10	0.174	CD38	9	31.09 ± 21.71%	51.20 ± 8.83%	43.20 ± 12.89%	39.88 ± 8.25%	54.99 ± 4.37%	50.07 ± 10.41%	39.58 ± 7.24%	58.97 ± 7.24%	63.59 ± 7.24%	2.23	4.39	<0.001	
CD4	13	20.91 ± 5.72%	20.54 ± 0.33%	35.78 ± 12.14%	31.06 ± 4.56%	33.28 ± 11.82%	41.19 ± 15.98%	37.25 ± 3.21%	1.94	6.24	0.259	CD4	11	21.71 ± 9.83%	60.88 ± 10.61%	23.53 ± 15.29%	35.25 ± 11.18%	43.16 ± 8.10%	44.57 ± 6.07%	33.93 ± 8.05%	41.78 ± 11.38%	43.45 ± 17.22%	3.58	2.04	0.002	
CD45	5	35.85 ± 8.76%	35.06 ± 1.75%	55.34 ± 16.75%	59.07 ± 3.54%	54.84 ± 25.63%	57.67 ± 13.96%	54.62 ± 3.91%	1.80	6.89	0.142	CD45	14	35.20 ± 23.80%	72.56 ± 10.89%	34.20 ± 26.84%	38.12 ± 12.61%	43.09 ± 18.46%	36.82 ± 9.29%	31.24 ± 13.36%	45.32 ± 12.65%	49.48 ± 26.32%	3.63	2.19	0.109	
CD69	3	52.84 ± 2.79%	51.87 ± 2.84%	52.92 ± 1.79%	48.76 ± 8.50%	57.52 ± 15.36%	59.66 ± 11.82%	57.06 ± 4.48%	1.37	1.19	0.749	CD69	1	29.67 ± 6.21%	50.28 ± 10.42%	24.20 ± 11.04%	27.35 ± 11.04%	17.81 ± 8.75%	30.71 ± 4.21%	24.42 ± 9.83%	39.68 ± 12.09%	47.65 ± 23.48%	3.31	2.46	0.007	
CD8	12	12.54 ± 3.89%	10.01 ± 0.74%	20.63 ± 8.72%	17.36 ± 1.79%	22.01 ± 15.96%	23.76 ± 11.82%	16.75 ± 3.21%	2.15	4.31	0.341	CD8	5	8.16 ± 26.01%	28.98 ± 9.07%	8.19 ± 7.74%	10.50 ± 4.17%	9.35 ± 5.45%	14.55 ± 2.99%	13.60 ± 8.61%	21.47 ± 8.61%	22.55 ± 14.21%	8.79	3.55	0.002	
FoxP3	7	39.41 ± 6.52%	39.26 ± 2.13%	59.41 ± 16.03%	62.86 ± 4.32%	57.05 ± 25.59%	60.68 ± 13.63%	57.55 ± 3.96%	1.78	7.62	0.157	FoxP3	10	41.92 ± 21.71%	79.52 ± 9.95%	48.24 ± 18.44%	55.38 ± 13.83%	75.93 ± 12.55%	61.89 ± 7.19%	49.96 ± 10.77%	69.78 ± 11.15%	66.16 ± 16.12%	2.15	3.77	0.001	
HLADR	15	37.14 ± 6.73%	34.60 ± 3.09%	48.30 ± 10.85%	46.44 ± 9.74%	49.46 ± 21.98%	52.34 ± 15.47%	49.08 ± 0.17%	1.44	4.13	0.505	HLADR	4	34.79 ± 29.50%	70.85 ± 19.80%	39.64 ± 22.67%	42.02 ± 14.58%	41.55 ± 17.19%	41.64 ± 10.38%	37.81 ± 14.18%	49.59 ± 19.49%	55.28 ± 24.27%	2.55	1.98	0.089	
Ki67	4	15.16 ± 4.31%	18.68 ± 1.01%	19.42 ± 2.68%	20.73 ± 4.19%	21.14 ± 3.40%	21.85 ± 3.40%	22.94 ± 4.79%	1.64	1.81	0.214	Ki67	8	21.16 ± 13.99%	19.60 ± 5.71%	20.08 ± 4.96%	22.75 ± 10.43%	26.34 ± 3.83%	29.15 ± 5.68%	18.57 ± 2.85%	21.03 ± 7.04%	22.97 ± 6.82%	1.55	2.45	0.391	

Figure 3: Comparison of 1mg/kg and 10mg/kg dosages across time points.

peak appeared by Day 64. These data suggest that 10 mg/kg induces strong immune modulation—with an early redistribution of cells into blood and a possible later increase from proliferation. This automated yet rigorous analysis reveals substantial insights into drug effects. A secondary response occurs beyond Day 64 for many markers. These data suggest that the 10mg/kg dosage is more immune modulating (compared to the 1mg/kg dose), and that activity occurs with a brief spike at Day 8, as well as a late response as far out as Day 85 (Figure 3). The other doses, including the intermediate dosages not shown, do not exhibit the strong Day 8 spike or the secondary Day 64–85 elevation. A quick (Day 8) increase in cells suggests redistribution of cells from the tissue into the peripheral blood (where the measurement was made) with a small persistent increase in cells at the later time points possibly arising from increased cell division at the intermediate time points. Furthermore, from this simple, yet rigorous analysis, a substantial understanding of drug effects can be attained.

terraFlow also generates box plots connecting individual patient

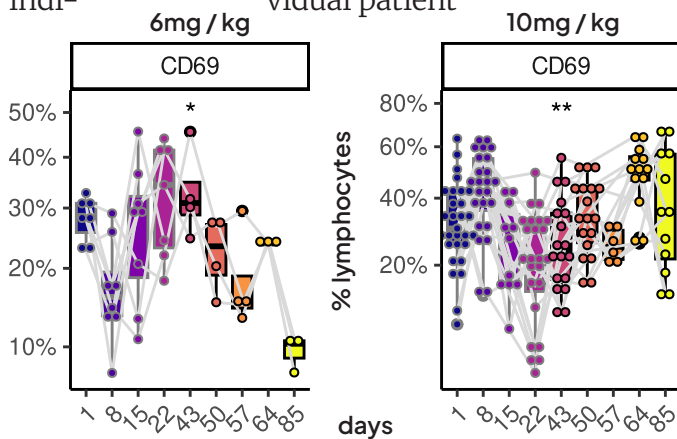


Figure 4: Changes in frequency of CD69+ cells between two dosages of drug.

data over time. Comparing 6 mg/kg and 10 mg/kg (Figure 4), a Day 8 spike in CD69+ cells is observed only at 10 mg/kg. CD69 levels drop at 6 mg/kg, including at Day 64, where they remain

elevated in the 10 mg/kg group. Other activation markers (HLA-DR, CD25, CD38) show similar dose-dependent patterns, confirming the drug's pharmacodynamic effect and dose sensitivity – two key elements of a pharmacodynamic analysis.

To further characterize dose response at 10 mg/kg, terraFlow performed an exhaustive phenotypic analysis based on marker combinations. Phenotypes were progressively filtered to retain only those with sufficient representation in the dataset, strong temporal stratification, and minimal redundancy. This refinement process ultimately yielded a small set of distinct, non-overlapping phenotypes that best represented dynamic changes over time (Figure 5).

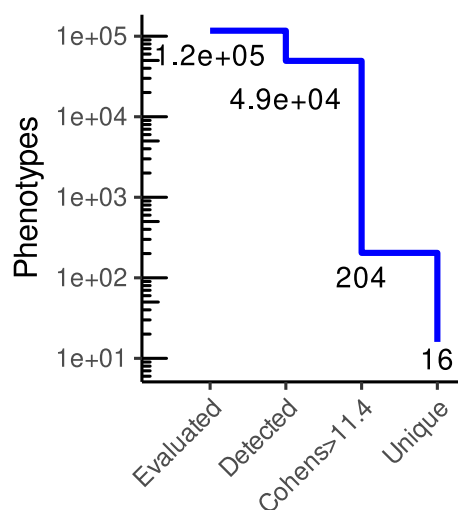


Figure 5: Stepwise refinement of phenotypes: 117,083 phenotypes were evaluated (rounded to 1.2e+05), of which 49,409 had sufficient event counts for analysis. Among these, 204 varied significantly across timepoints (Cohen's $d > 1.4$), and 16 were unique, non-overlapping phenotypes.

From these 204 phenotypes, a machine learning model was built using 10-fold cross-validation. On each fold, 90% of samples trained a logistic regression model using selected phenotypes; the model then classified the remaining 10%. The accuracy of the model was scored using an AUC (Area under the ROC Curve) value, which reflects the model's ability to distinguish between comparison groups. AUC score values range from 0 to 1 with a higher ROC AUC indicating

a better performance. A perfect model would have an AUC of 1, while a random model would have an AUC of 0.5. This process tested whether phenotypes reliably captured treatment-related differences. Sensitivity/specificity curves and AUC values were calculated (Figure 6), with AUCs of 0.90–1.00 at several time points (e.g., Days 1, 8, 15, 43, 50, 57, and 85), highlighting them as ideal for further investigation.

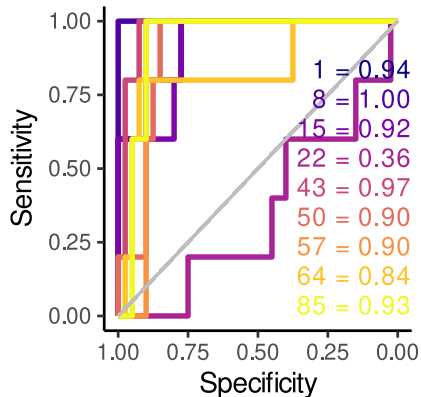


Figure 6: AUC curves showing how well the model of significant phenotypes predicts each time point in treatment.

The day 8, 64, and 85 time points are worth further examination, since so many of the markers studied had elevated expression (Figure 3) and strong dose-dependent differences were observed (Figure 4) at these time-points. A stand-out combinatorial phenotype was the CD38+ CD127- CD314+ PD1+ Ki67- cell population identified and validated in the platform, which tracked strongly with treatment (Figure 7). terraFlow provided an expanded view of this cell population as well. Although these markers are not needed by the model to classify time-points, terraFlow also provided further functional context, showing these cells were predominantly HLA-DR+ (92.3% of the reported cells), FoxP3+ (100% of reported cells), and CD25+ (99.4% of reported cells, data not shown, but presented in the automated report)—indicating an exhausted, possibly cytolytic T-cell subset.

Interpretation of dose-dependent cell types

terraFlow matched identified phenotypes to published literature, providing functional context. For example, CD38+ PD1+ CD127- cells are known to be exhausted and often co-express CTLA4 and TIM3 (Cai et al., Nature Communications 13, 7543 (2022)). CD314+ cells—also part of the phenotype—are broadly cytolytic across a wide variety of settings. These findings suggest the drug induces cytolytic T-cells that cannot proliferate and are destined for exhaustion. Interestingly, these cells showed two peaks: one 8 days after treatment initiation and another after 64+ days. A critical question for future study is whether these exhausted cells are enriched in non-responders. Although these cells represent a minor fraction of PBMC, they are compelling for their functional traits.

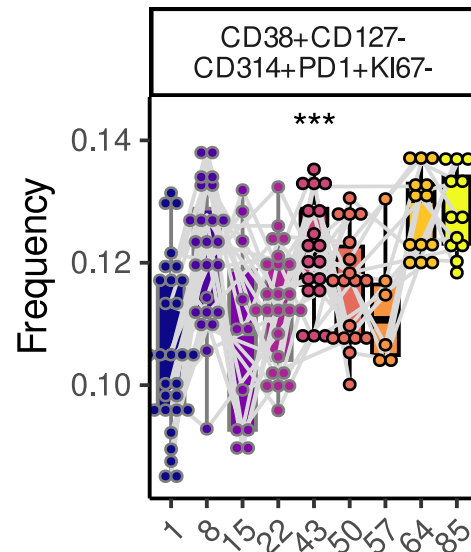


Figure 7: Frequency of model identified cell population over treatment.

Activated (CD69+) T-cells represent most cells modulated in a dose-dependent manner over the course of treatment, though there is a wide variation in expression amongst patients, supporting the hypothesis that differences in this marker might explain differences in treatment outcome.

Summary

In this paper, we demonstrated how a simple upload of FCS files to terraFlow can reveal drug mechanisms, dose-response relationships, and inter-individual variability. The platform identified precise immune phenotypes, informative time points, and biologically meaningful trends—all linked to literature references that help guide future research.

Specifically, this analysis reveals time points most reliable for study, the specific markers in the panel that warrant future study, along with potential functional traits gleaned from the contextualizing of findings within an automated literature search. terraFlow's approach is vastly different from older methods that track only a few cell types, lack analytical rigor, or require extensive manual tuning. Its power lies in exhaustive, unbiased analysis, high-resolution phenotype identification, and contextual grounding in the scientific literature—empowering researchers to uncover new insights and drive their next breakthrough.

